Available online at www.sciencedirect.com
SCIENCE DIRECT
Catalysis Today 115 (2006) 80–87
CATALYSIS TODAY
www.elsevier.com/locate/cattod

Direct synthesis of dimethyl carbonate with supercritical carbon dioxide: Characterization of a key organotin oxide intermediate

Danielle Ballivet-Tkatchenko [a,*], Stéphane Chambrey [a], Riitta Keiski [b], Rosane Ligabue [a], Laurent Plasseraud [a], Philippe Richard [a], Helka Turunen [b]

[a] *LSEO, UMR 5188, CNRS-Université de Bourgogne, BP 47870, 21078 Dijon Cedex, France*
[b] *Department of Process and Environmental Engineering, P.O. Box 4300, 90014 University of Oulu, Finland*

Available online 11 April 2006

Abstract

The direct synthesis of dimethyl carbonate (DMC) using carbon dioxide as solvent and reagent for its fixation to methanol was explored with di-*n*-butyldimethoxystannane in order to get insight into the reaction mechanism for activity improvement. Catalytic runs including recycling experiments allowed isolation and characterization by NMR, IR, and single-crystal X-ray diffraction of a new tin complex containing 10 tin atoms. This compound could be prepared independently and is considered as a resting species. The yield of DMC is highest under 20 MPa pressure that fits with a monophasic supercritical medium in agreement with fluid phase equilibria calculations. In line, preliminary kinetics and initial rate determination show a positive order in carbon dioxide and a first-order dependence on the stannane. The initial rates were lower with the deca-tin complex than with the stannane precursor, but the turnover numbers (TONs) were higher. Water, the co-product of the reaction, was found to reversibly poison the active centers. Its in situ trapping had a beneficial effect. This study provides new mechanistic clues as to the reactive species and DMC formation. Further kinetics work is in progress to determine the rate-limiting step(s) at the initial stage of the reaction for more active catalyst design.

Keywords: Dimethyl carbonate; Dibutyldimethoxystannane; Organotin oxide; Supercritical carbon dioxide; Carbon dioxide–methanol phase diagrams

1. Introduction

The chemical utilisation of carbon dioxide could contribute to closing the global CO_2-cycle, and allow carbon dioxide to be viewed as a renewable feedstock [1,2]. In the past decade, reports on the use of carbon dioxide as solvent for chemical synthesis have expanded, motivated by the implementation of benign processes [3,4]. As a matter of fact, supercritical carbon dioxide ($scCO_2$) exhibits physicochemical properties amenable for replacing volatile organic solvents. Its critical parameters are easily accessible experimentally ($P_c = 7.38$ MPa, $T_c = 304.2$ K, $d_c = 0.468$ g mL^{-1}) and its solvent properties tunable by adjusting temperature and pressure [5]. Both organometallic and heterogeneous catalysts have been studied under these conditions. Rate and selectivity enhancements may be effective due to switching rate-limiting step(s) under monophasic conditions and pressure [6–9]. On the opposite, emerging strategies take advantage of multiphasic conditions under which the catalyst is insoluble in the $scCO_2$-rich phase and the reaction products soluble. Therefore, coupling reaction and separation steps in a single reactor would facilitate recycling operations of the catalyst. Moreover, such an immobilization of organometallics is suitable for continuous-flow operation under multiphasic conditions. Recent research in this area points out that ionic liquids–$scCO_2$ biphasic systems are good candidates for emissionless processes [10–13].

A particular use of $scCO_2$ is as solvent and reagent. Under these conditions, $scCO_2$ becomes an excellent medium for its own hydrogenation to formic acid derivatives, with catalysts exhibiting turnover numbers (TON) and frequencies (TOF) higher than any previously reported for subcritical systems [14–17]. Interestingly, both ruthenium-based complexes and hybrid gels proved to be the most active affording, for example, TOFs up to 360,000 h^{-1} in *N*,*N*-dimethylformamide synthesis [18]. The irreversibility of the reaction, under the conditions used, is a favorable factor for achieving the outstanding performances

* Corresponding author. Tel.: +33 3 80 39 37 70; fax: +33 3 80 39 37 72.
E-mail address: ballivet@u-bourgogne.fr (D. Ballivet-Tkatchenko).

0920-5861/$ – see front matter © 2006 Elsevier B.V. All rights reserved.
doi:10.1016/j.cattod.2006.02.025

[19]. The other relevant examples taking benefits from $scCO_2$ as a C1 synthon are found for the synthesis of cyclic carbonates [20,21] and dimethyl carbonate (DMC) [22–28].

DMC has expanded in production volume as its uses have evolved from specialty applications [29] to larger scale for phosgene-free polycarbonate and polyurethane productions [30]. DMC has also been mentioned as a possible gasoline blending component [31] with low toxicity, rapid biodegradability [32] and low impact on air quality [33]. DMC is currently produced by two routes. The phosgene route [34] exhibits inherent hazard and environmental issues in handling highly toxic chemicals and in waste disposal. The second route, the catalytic oxidative carbonylation of methanol [35,36], offers operational and environmental advantages. However, scale-up production would not be effective with these existing technologies. Therefore, the search for benign by design synthesis has been the impetus for research involving CO_2 [37]. Currently, the three reaction pathways of interest are (i) transesterification between cyclic carbonate and methanol (Eq. (1)); (ii) urea methanolysis (Eq. (2)); and (iii) direct carbonation of methanol (Eq. (3)). On a stoichiometric basis, the direct carbonation appears more attractive because the atom efficiency [38] is highest, 83 wt%, forming only 17 wt% of water as the co-product versus 41 wt% of glycol for transesterification (Eq. (1)). But it still suffers from poor catalyst activity. Clearly, further research advancements are needed for practical assessment. One of the keys to accomplishing this goal is the rational design of improved catalysts based on mechanism understanding. Few publications discuss possible catalytic cycles, which require a set of convincing experiments to be exploited [39–41]. Among the precursors reported so far, organometallic tin (IV) complexes exhibit higher selectivity [22–28,41]. The other advantage resides in structural information from ^{119}Sn NMR spectroscopy.

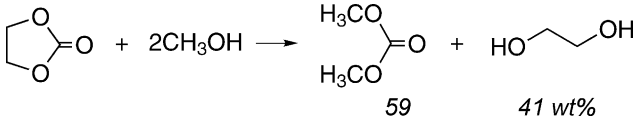

(1)

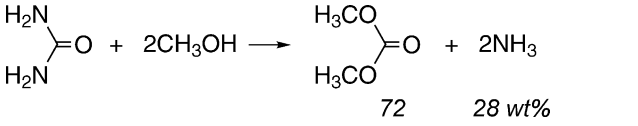

(2)

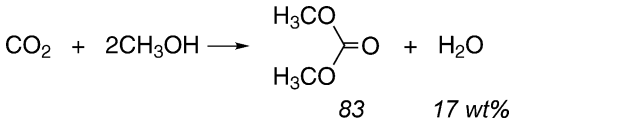

(3)

The aim of the study herein reported is to present mechanistic information on reaction (3) using CO_2 as solvent and reagent in the presence of di-*n*-butyldimethoxystannane. Multinuclear NMR, IR, and X-ray techniques have provided insight into species present under catalytic conditions. A new organotin oxide complex could be isolated, characterized and likely identified as a resting species. The first preliminary investigation of the kinetics in modifying tin concentration, temperature, and pressure is presented in order to elucidate the positive effect of $scCO_2$. It was, therefore, also necessary to acquire informations on the *P–T* phase diagrams for the relevant binary methanol–CO_2 mixtures. This could be successfully achieved through calculations and visual experiments with a reactor equipped with sapphire windows.

2. Experimental

2.1. General procedures

All manipulations were carried out by using standard Schlenk techniques [42]. Toluene and methanol (Carlo Erba, RPE grade) were dried and distilled under argon from CaH_2 and $Mg(OCH_3)_2$, respectively. Carbon dioxide N45 TP purchased from Air Liquide was used without further purification. The compounds *n*-$Bu_2Sn(OCH_3)_2$ and [*n*-$Bu_2(CH_3O)Sn]_2O$ were synthetized according to published methods [28].

The NMR spectra were recorded at 295 K in $CDCl_3$ on a Bruker Avance 300 spectrometer (^{1}H = 300.131, ^{119}Sn = 111.910, and ^{13}C = 75.475 MHz). ^{1}H and ^{13}C chemical shifts (δ, ppm) were determined relative to the solvent ($CHCl_3$ δ 7.24, $CDCl_3$ δ 77.00) and converted to the scale downfield from $(CH_3)_4Si$. ^{119}Sn{^{1}H} chemical shifts (δ, ppm) are reported downfield from $(CH_3)_4Sn$, as the internal standard. IR spectra were recorded on a Bruker Vector 22 equipped with a Specac Golden Gate™ ATR device. Elemental analysis was performed at the Laboratoire de Synthèse et Electrosynthèse Organométalliques, Université de Bourgogne, Dijon.

2.2. Experiments under pressure

Caution: since high pressures are involved, appropriate safety precautions must be taken.

Typical procedure for reaction: the reaction was carried out in a 125-mL stainless steel reactor equipped with a magnetic stirrer. The reactor was purged with argon, and a 20 mL solution of the tin complex (4 mmol) in methanol was introduced by syringe. Then, CO_2 was admitted to the desired amount with an ISCO 260D pump. The reaction temperature was controlled by an internal thermocouple. After a given reaction time, the reactor was cooled down to 273 K, pressure was gently released, and the liquid phase was transferred to a Schlenk tube. Trap-to-trap distillation under vacuum at room temperature allowed separation of volatile compounds that were quantitatively analyzed by GC (benzene as internal standard, Fisons 8000, J&W Scientific DB-WAX 30 m capillary column, FID detector). Tin residue was characterized by multinuclear NMR and IR. Recycling experiments consisted of taking the tin residue for successive runs under the same experimental conditions.

For the kinetic experiments, a 56-mL reactor was used and charged with a 9-mL solution of the tin complexes (0.1–2.5 mmol). A sampling valve (0.090 mL) was used to follow the DMC yield with time. At the end of the experiment, the aforementioned degassing and analytical procedures were adopted. Before quenching the reaction at 273 K, a last sampling was performed to check consistency between the two analytical procedures; the fit was better than 3% (relative error).

2.3. X-ray crystallography on $(n\text{-}Bu_2SnO)_6[(n\text{-}Bu_2SnOCH_3)_2(CO_3)]_2$

Colorless needle crystals suitable for X-ray diffraction analysis were grown from a methanol solution of the residue arising from a recycling run. Crystal data: $C_{86}H_{192}O_{16}Sn_{10}$, $M = 2669.56$; triclinic; $a = 13.4502(3)$, $b = 14.2594(3)$, $c = 16.8905(4)$ Å, $\alpha = 69.244(1)$, $\beta = 77.519(1)$ and $\gamma = 76.366(2)^\circ$; $V = 2912.36(11)$ Å^3; $T = 180$ K, space group P-1. The structure was solved by direct methods but unfortunately, the butyl groups attached to the tin atoms were severely disordered and only the planar core of the ladder was successfully refined. Selected bond lengths and angles are given in the supplementary material.

2.4. Synthesis of $(n\text{-}Bu_2SnO)_6[(n\text{-}Bu_2SnOCH_3)_2(CO_3)]_2$

An equimolar mixture of *n*-Bu_2SnO (2.652 g, 10.65 mmol) and dimethyl carbonate (0.958 g, 10.65 mmol) in toluene (25 mL) in the presence of methanol (0.2 mL) was heated in a sealed vial at 398 K. After ca. 30 min, the suspension turned to a clear solution and heating was continued for 1 h. After cooling down to room temperature, filtration and removal of the volatiles under vacuum, left a white sticky solid. Several washings with aliquots of methanol (5 mL) led to a fine white powder characterized as the title compound. Yield: 2.491 g (86%). $^{119}Sn\{^1H\}$ NMR, δ: −171.2 ($^2J(^{119}Sn,^{119}Sn) = 204$ Hz, $^2J(^{119}Sn,^{117}Sn) = 197$ Hz), −177.7 ($^2J(^{119,117}Sn,^{119,117}Sn) = 240$, 106 Hz), −233.9 ($^2J(^{119,117}Sn,^{119,117}Sn) = 199$, 106 Hz, $^1J(^{119}Sn,^{13}C) = 683$ Hz). ^1H NMR, δ: 3.27 (12H, OCH_3), 1.8–0.8 (180H, butyl). $^{13}C\{^1H\}$ NMR, δ: butyl chain Cα 23.52 ($^1J(^{13}C,^{119}Sn) = 642$ Hz, $^1J(^{13}C,^{117}Sn) = 614$ Hz), 22.07 ($^1J(^{13}C,^{119}Sn) = 681$ Hz, $^1J(^{13}C,^{117}Sn) = 651$ Hz), 21.23 ($^1J(^{13}C,^{119}Sn) = 619$ Hz, $^1J(^{13}C,^{117}Sn) = 591$ Hz), Cβ,γ 28.05, 27.85, 27.49, 27.40, 27.24, and 27.16, Cδ 14.00, 13.65, 13.63, methoxy 50.78, carbonate 163.68. IR (neat): ν (CHmethoxy) 2801 cm^{-1}, ν (CO_3) 1539 (s), 1373 (vs) cm^{-1}. Anal. Calcd. for $C_{86}H_{192}O_{16}Sn_{10}$ (2669.56): C, 38.69; H, 7.25. Found: C, 38.98; H, 7.09%.

2.5. Phase behavior observation

A fixed-volume reactor (46 mL) equipped with sapphire windows (Top Industries S.A., France), a magnetic stirrer, and temperature and pressure gauges was charged with methanol (5.69 g, 178 mmol) and optionally with the tin complexes (1 mmol, based on tin), DMC and H_2O (1 mmol), then pressurized with CO_2 to the desired amount with an ISCO 260D pump at room temperature. The temperature was gradually increased up to the visual disappearance of the liquid meniscus. It was, then, adjusted and stabilized for 3 h in order to observe the transition between a non-transparent and a transparent monophasic medium upon regulation at ±1 K. The pressure was measured within an accuracy of ±0.1 MPa.

3. Results and discussion

3.1. DMC yield from $n\text{-}Bu_2Sn(OCH_3)_2$ and recycling experiments

The precursor *n*-$Bu_2Sn(OCH_3)_2$ led to the highest DMC yield at 423 K, according to reaction (3). Above this temperature, redistribution of the butyl ligands was observed on the $^{119}Sn\{^1H\}$ NMR spectrum of the residue after work-up of the solution. Increasing gradually CO_2 pressure from 9 to 20 MPa improved significantly DMC yield. Further pressure increase up to 25 MPa had no beneficial effect. The reaction times are quite lengthy, being more than 24 h, to obtain a maximum yield corresponding to a DMC:Sn molar ratio close to 1. The selective formation of the organic carbonate versus dialkyl ether was confirmed from *n*-$Bu_2Sn(OCH_2CH_3)_2$ precursor, because diethyl ether could be more easily quantified than dimethyl ether, if any. Diethyl carbonate was formed similarly to DMC, whereas diethyl ether was not detected by GC-MS.

After a typical run at 20 MPa, the NMR and IR fingerprints of the organometallic residue were no more those of the starting compound. Interestingly enough, the organometallic residue was still active for DMC formation for several recycling experiments as evidenced in Fig. 1 (runs 2–7). The DMC yield was quite constant but lower than with the fresh *n*-$Bu_2Sn(OCH_3)_2$ precursor. After run 7, a blank test performed without the tin compound (run 8) showed no residual activity of the reactor. Reloading the tin residue in the presence of 2,2-dimethoxypropane (DMP, 10 mmol) had a promoting effect (run 9) that could be enhanced when conducting the reaction over a longer time (96 h, run 10). Acetone was also formed

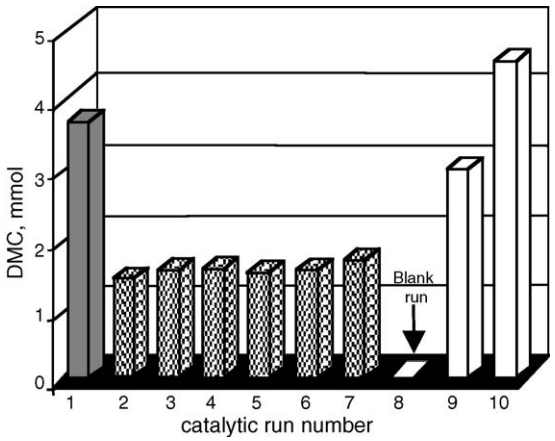

Fig. 1. DMC yield vs. number of successive catalytic runs under 20 MPa for 15 h at 423 K: (1) *n*-$Bu_2Sn(OCH_3)_2$, 4 mmol; (2–7) successive recyclings from (1); (9) addition of DMP 10 mmol; and (10) addition of DMP 10 mmol, $t = 96$ h (for each run: $CH_3OH = 0.50$ mol, $CO_2 = 0.82$ mol).

during this reaction, pointing out that DMP was a water-trapping agent (Eq. (4)), as already reported in a similar approach [25]. Therefore, the turnover-limiting step appears to be the consequence of the accumulation of water according to reaction (4). It is noteworthy that, under these conditions, DMC yield does not reach the thermodynamic equilibrium of reaction (3). The principal hindrance resides in the poisoning of the active species, in agreement with our previous study on the use of $Si(OCH_3)_4$ as a methoxy transfer reagent making the reaction catalytic [28].

(4)

Our efforts to characterize the tin residue after recycling runs in the presence of methanol were finally successful. Single crystals, suitable for X-ray analysis and structure determination, could be grown from a methanolic solution of the residue.

3.2. X-ray structure and NMR characterization of the deca-tin complex (n-$Bu_2SnO)_6[(n$-$Bu_2SnOCH_3)_2(CO_3)]_2$

The overall structure could not be satisfactorily refined due to highly disordered *n*-butyl groups. We have not yet succeeded to obtain better structure refinement despite many attempted measurements at several temperatures and from different mother solutions. However, such disorder of the butyl groups is not of prime importance for the present structural discussion.

The molecular structure is based on 10 tin atoms, each of them displaying a distorded trigonal–bipyramidal coordination (Fig. 2a). All the tin centers bear two *n*-butyl groups, showing that the $C(sp^3)$–Sn bonds are stable under the reaction conditions. The corresponding carbon atoms bonded to tin are located in the equatorial plane. Three trigonal–bipyramidal tin environments are revealed. The first one corresponds to n-Bu_2SnO_3 (O tricoordinate mode, μ_3), the second to n-$Bu_2Sn(\mu_3\text{-}O)_2(\mu_2\text{-}OCH_3)$ as encountered in distannoxanes, and the third to n-$Bu_2Sn(\mu_3\text{-}O)_2(\mu_2\text{-}OCH_3)(\mu_2\text{-}CO_3)$. The molecule is centrosymmetric with a planar $Sn_{10}O_6(OCmethyl)_4(CO_3)_2$ core; the RMS deviation is equal to 0.06 Å from the mean plan containing the 32 core atoms (Fig. 2b). The general connectivity of the backbone involves tin–oxygen bonds, the lengths of which are, as expected, shorter in the equatorial plane than in the axial positions. The deca-tin complex can be viewed as a pair of coplanar ladders of (n-$Bu_2Sn)_5O_5$ consisting of four four-membered rings linked together by two carbonate groups acting as μ_1, μ_1-bridging ligands. Moreover, for these two carbonate ligands the planar syn–syn conformation is stabilized. The corresponding Sn(1)–O(6) and Sn(5#)–O(7) bond lengths are equivalent within experimental error at 2.111(6) Å and the Sn(1)...Sn(5#) distance is 5.68 Å. The internal 16-membered ring thus created has an opening dimension of 5.47 (O(6)...O(7#)) by 6.12 (Sn(3)...Sn(3#)) Å, potentially suitable for host–guest chemistry involving small molecules. Interestingly enough, both carbonate and methoxy ligands are present on the periphery, that is most probably reminiscent of DMC formation. The bridging methoxy groups are slightly different with O–Sn distances of 2.239(7), 2.164(7), 2.295(7) and 2.148(7) Å for O(1)–Sn(1), O(1)–Sn(2), O(5)–Sn(5) and O(5)–Sn(4), respectively. This compound is the first example of a high-nuclear *n*-butyltin oxide framework in a planar arrangement. While our work was in progress, an X-ray structure of a dibenzyl (Bz) analogue was published [43]. The compound formulated as $[(Bz_2SnO)_3(Bz_2SnOH)(Bz_2SnOCH_2CH_3)(CO_3)]_2$ is also a deca-tin compound, but bearing two hydroxyl and ethoxy groups instead of four methoxy groups.

To obtain additional evidence that the isolated complex is not a side product formed during crystallization from the residue, we performed and optimized its synthesis via classical organometallic routes (yield >80%) for testing the reactivity on authentic samples. The single-crystal X-ray structure determination and multinuclear NMR spectra nicely confirmed that we deal with the same compound.

The ^1H, ^{119}Sn, and ^{13}C NMR spectra in solution could not reveal the exact oligomeric structure. However, the following features are in full agreement with a decanuclear species,

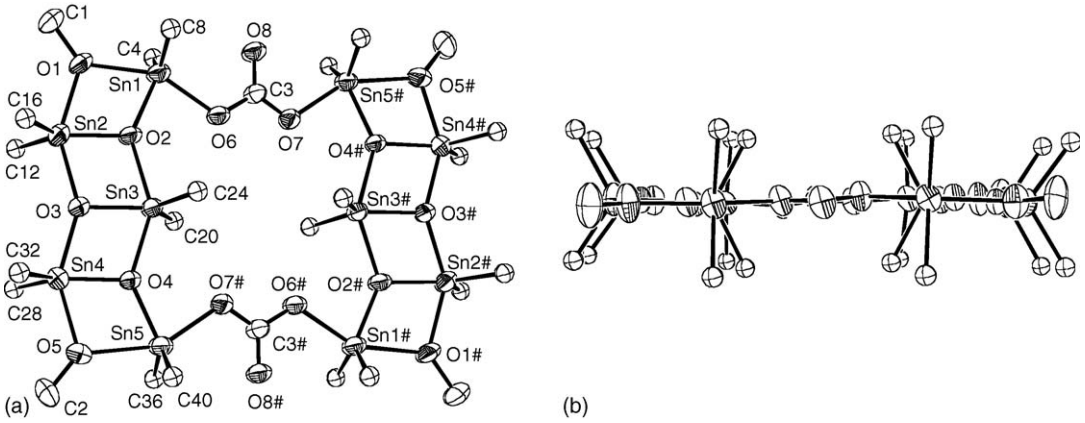

Fig. 2. ORTEP view of the molecular structure of (n-$Bu_2SnO)_6[(n$-$Bu_2SnOCH_3)_2(CO_3)]_2$: (a) with crystallographic numbering scheme and (b) planearity of the $Sn_{10}O_6(OC_{methyl})_4(CO_3)_2$ core (for clarity the hydrogen atoms are omitted and only the butyl carbon atoms linked to the tin centers are shown due to the disordered butyl chains).

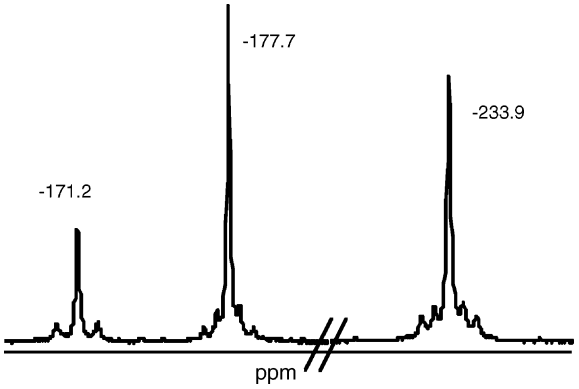

Fig. 3. $^{119}Sn\{^1H\}$ NMR spectrum of $(n\text{-}Bu_2SnO)_6[(n\text{-}Bu_2SnOCH_3)_2(CO_3)]_2$ in $CDCl_3$ at 295 K.

suggesting that the solid structure is retained in $CDCl_3$ solution. The ^1H spectrum showed one signal at δ 3.27 (OCH_3) and a massif between 1.8 and 0.8 (*n*-butyl groups) with the relative integration OCH_3:butyl ratio of 2:10. The $^{119}Sn\{^1H\}$ NMR spectrum shown in Fig. 3 displayed three resonances at δ −171.2, −177.7, and −233.9 (relative integration 1:2:2), well in the range of five-coordinated tin atoms [44]. The $^{13}C\{^1H\}$ spectrum exhibited the signature of carbonate and methoxy groups at δ 163.68 and 50.78, respectively, in agreement with the IR fingerprint (ν (CO_3): 1539 and 1373 cm^{-1}, ν (OC–H): 2801 cm^{-1}). Three resonances for the α carbon atoms of the butyl chains were found at δ 23.52, 22.07, and 21.23 (relative integration 1:2:2). Six resonances in the range δ 28.05–27.16 were present due to the β and γ carbon atoms of the butyl chains, and three at 14.00, 13.65, and 13.63 for the δ ones. Therefore, three different environments were identified for the tin centers, each of them surrounded by two equivalent butyl chains. Four methoxy groups per 10 Sn atoms were found. Moveover, $^{119,117}Sn$ couplings could also be measured on the $^{119}Sn\{^1H\}$ and $^{13}C\{^1H\}$ spectra that allowed further assignments (see Section 2).

3.3. Fluid phase equilibria

As the catalytic runs were performed at pressure and temperature beyond the critical point of CO_2 (P_c = 7.38 MPa, T_c = 304.2 K) and below that of CH_3OH (P_c = 8.10 MPa, T_c = 512.6 K) [45], it was of relevance to determine whether the reaction takes place under monophasic or multiphasic conditions. The nature and number of phases may account for the pressure effect described in Section 3.1 by changing the relative concentrations and, therefore, the kinetics.

Phase equilibrium data on binary mixtures of methanol–carbon dioxide are available in the literature either from measurements [46–48] or calculations [49]. However, they did not provide straightforward values for the pressures, temperatures, and binary compositions used in this work. Moreover, we could notice from different sources deviations larger than the experimental uncertainties [48,49]. We, therefore, decided to run calculations and experiments directly applicable to our own study. The *P–T* phase diagrams were calculated to determine two-phase, liquid, vapour, and supercritical fluid domains for the binary methanol–carbon dioxide mixture. Calculations were done with the Flowbat simulation program [50] using the Soave-Redlich-Kwong equation of state [51,52]. The phase envelopes thus obtained (Fig. 4) show that decreasing CO_2 mol% from 97 to 24 leads to drastic changes in monophasic–biphasic boundaries. The critical points for each composition are also shown in Fig. 4 (filled squares). The line drawn through these calculated critical points (Fig. 4, dashed line) points out that the corresponding pressures pass through a maximum at 67.35 CO_2 mol% (P_c = 16.61 MPa, T_c = 412.94 K), while the critical temperature increases monotonically with the methanol content. It is noteworthy that the maximum critical pressure value is much higher than those of the pure components.

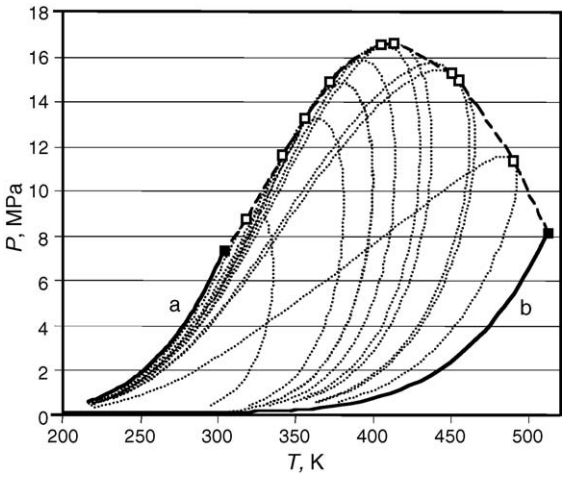

Fig. 4. Calculated *P–T* diagrams for liquid–vapor coexistence curves and critical points for binary CO_2–CH_3OH mixtures: (–) liquid–vapour line for (a) CO_2, (b) CH_3OH; (. . .) two-phase liquid–vapor envelope for binary mixture compositions, from left to right: 97.1, 89.4, 84.04, 78.6, 71.3, 67.35, 51.78, 49.2, 24.4 CO_2 mol%, respectively; (■) CP for (a) CO_2, (b) CH_3OH; (□) CPs of the binary mixtures; and (- - -) binary mixtures critical line.

The observed increase in DMC yield with CO_2 pressure correlates nicely with the calculated phase changes from a two-phase to a one-fluid area, i.e. from 9 (46 CO_2 mol%) to 25 MPa (70 CO_2 mol%) at 423 K. However, the purity of the chemicals used for the reaction may exert significant influence on the phase equilibrium data. In addition, the chemical composition changes under batch conditions. DMC and water are accumulating as the reaction proceeds and tin compound is also present, although they remain at low levels (<1 mol%). Because modeling was not realistic due to the multicomponent nature of the system, we visually checked the phase behavior in performing the reaction in a batch reactor equipped with sapphire windows. A CO_2 loading in the range 69.7–64.8 mol% allowed to reach a final pressure >16 MPa at 423 K. While heating, the change to a one-phase regime was systematically observed when the pressure reached 16.2 ± 0.1 MPa. The corresponding temperature was more sensitive to the CO_2 loading, following the same trend as that depicted Fig. 4. The good fit obtained between calculation and visual inspection allowed us to set the pressure at either 10 or 20 MPa for the kinetic study for comparing the performance under biphasic and monophasic conditions in the temperature range 373–423 K.

3.4. Kinetic study

In order to get a better understanding of the reaction mechanism, a comparative kinetic study of reaction (3) was undertaken with n-$Bu_2Sn(OCH_3)_2$ and $(n\text{-}Bu_2SnO)_6[(n\text{-}Bu_2Sn(OCH_3)_2)(CO_3)]_2$. For clarity, the abbreviation used in the following for the two compounds will be Sn-1 and Sn-10, respectively. The preliminary experiments herein reported focus on the temperature onset of measurable initial rates under biphasic (10 MPa) and monophasic (20 MPa) conditions, and on the role of methanol on the kinetic profiles. For that purpose, methanol was substituted for toluene in order to determine whether the methoxy ligands of both compounds are prompted to form DMC under CO_2 pressure, and, if so, to determine the stoichiometry and the partial order in tin.

Sn-1 exhibited a measurable activity versus time at 355 K. Fig. 5 shows typical profiles of DMC yield under 10, 20, and 24 MPa at 387 K. During the first hours of a run, the reaction rate is constant which allows accurate initial r_0 determinations for $t = 0$. Moreover, a rate enhancement is clearly observed from 10 to 20 MPa with r_0 values of 0.95×10^{-3} and 3.9×10^{-3} mol h^{-1} per Sn (mol L^{-1}), respectively, that suggests a positive order in CO_2. A further increase to 25 MPa had no effect, matching with our previous results at 15 h reaction times (Section 3.1). Interestingly, replacing methanol for toluene did not suppress DMC formation (Fig. 5). The calculated r_0 of 1.1×10^{-3} mol h^{-1} per Sn (mol L^{-1}), compares well with that obtained with methanol at the same biphasic conditions (10 MPa).

Whatever the pressure, the maximum yield in DMC corresponds to a DMC:Sn molar of ~0.5. An increase in temperature shortens the time for reaching the plateau. The resulting tin residue was identified as the distannoxane $[n\text{-}Bu_2(CH_3O)Sn]_2O$ by comparing the multinuclear NMR and IR spectra, and elemental analysis with an authentic sample previously prepared [28]. The outcome of these experiments is the overall stoichiometry depicted in Eq. (5). In order to determine whether reaction (5) involves a mononuclear or a binuclear mechanism, the reaction order with respect to Sn-1 was calculated from the r_0 values by the differential method. The tin concentration was varied over the range 0.07–0.2 mol L^{-1}, and temperature and pressure set at 9 MPa and 371 K, respectively. Under these conditions, the molar ratio of dissolved CO_2 to Sn-1 was estimated to be >40, according to published data on liquid–vapor equilibria of CO_2–toluene mixtures [53]. Plotting ln r_0 versus ln [Sn-1] showed a linear dependence with a slope of 1.02 ± 0.01 corresponding to the partial order in Sn-1. This first-order behavior strongly suggest that DMC formation involves the mononuclear n-$Bu_2Sn(OCH_3)_2$ complex. At first glance, this is not too surprising as the presence of two methoxy ligands may afford DMC under CO_2. However, the resulting tin compound should correspond to n-Bu_2SnO, which is not the isolated species. In fact, we have found that n-Bu_2SnO easily reacts with n-$Bu_2Sn(OCH_3)_2$ in the same temperature range to form quantitatively the distannoxane $[n\text{-}Bu_2(CH_3O)Sn]_2O$, rationalizing reaction (5) stoichiometry. Further work is in progress for determining the reaction order with respect to CO_2 and the activation energy of the reaction. At this stage, it appears that an intramolecular mechanism operates from precursor Sn-1 and does not imply methanol as a reactant. Of course, methanol is a prerequisite for catalysis to proceed and under these conditions a resting Sn-10 species has been isolated and characterized.

$$2n\text{-}Bu_2Sn(OCH_3)_2 + CO_2 \rightarrow [n\text{-}Bu_2(CH_3O)Sn]_2O + DMC \quad (5)$$

At the same tin loading, Sn-10 exhibited measurable initial rates at 398 K, a much higher temperature than 355 K for Sn-1. At this point, we can speculate that the rate-limiting steps are distinct. As a matter of fact, no activity was found in toluene contrasting with Sn-1. Nevertheless, in the presence of methanol Fig. 6 shows also a clean rate enhancement with CO_2 pressure from 11 to 22 MPa with r_0 values of 0.75×10^{-3} and 2.9×10^{-3} mol h^{-1} per Sn (mol L^{-1}) at 411 K, respectively.

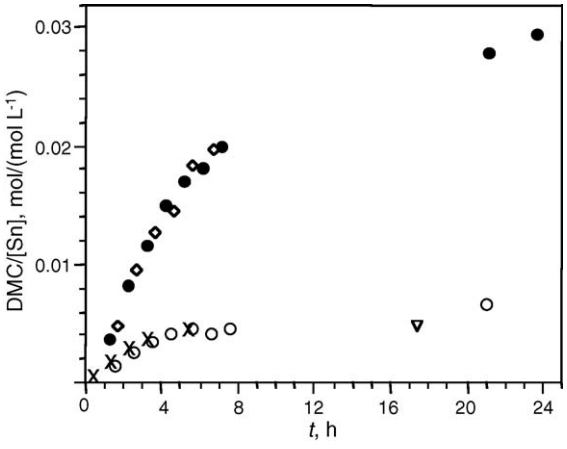

Fig. 5. DMC yield as a function of reaction time and CO_2 pressure with n-$Bu_2Sn(OCH_3)_2$ at 387 K: (○) 10 MPa, mmol $CH_3OH/CO_2/Sn$ = 232/234/1.44; (◇) 20 MPa, mmol $CH_3OH/CO_2/Sn$ = 227/490/1.42; (●) 24 MPa, mmol $CH_3OH/CO_2/Sn$ = 225/556/1.50; (×) 9 MPa, mmol toluene/CO_2/Sn = 78/230/1.52.

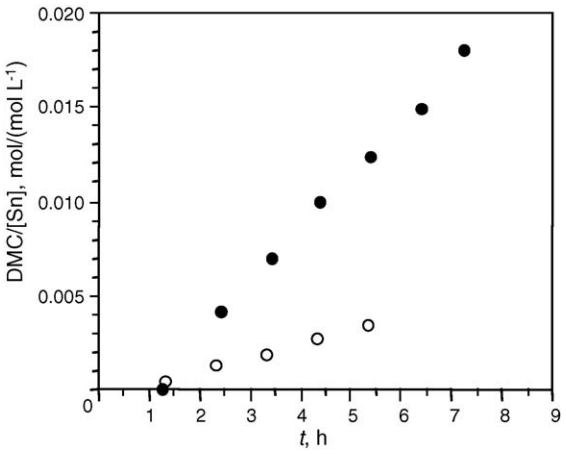

Fig. 6. DMC yield as a function of reaction time and CO_2 pressure with $(n\text{-}Bu_2SnO)_6[(n\text{-}Bu_2SnOCH_3)_2(CO_3)]_2$ at 411 K: (○) 11 MPa, mmol $CH_3OH/CO_2/Sn$ = 227/221/0.87; (●) 22 MPa, mmol $CH_3OH/CO_2/Sn$ = 225/478/0.83.

The initiation period close to 1 h may be assigned, at first, to the heating time for equilibrating the reaction temperature, although further chemical transformation cannot be discarded.

The activity of Sn-10 only revealed under methanol leads to consideration of its chemical composition and structural arrangement. There are a number of ways for viewing the building blocks due to the high nuclearity. At the present stage of our knowledge, we can only speculate in proposing the formula as $(n\text{-}Bu_2SnO)_6[(n\text{-}Bu_2SnOCH_3)_2(CO_3)]_2$, which is somehow reminiscent of the distannoxane structure $[n\text{-}Bu_2(CH_3O)Sn]_2O$. However, the Sn–O–Sn bond was found to be reluctant to CO_2 fixation. Carbon dioxide was only inserted into the Sn–OCH_3 bond leading to a hemicarbonate $SnOC(O)OCH_3$ fragment [28]. The common feature between Sn-10 and the distannoxane is the presence of only one methoxy group linked to one tin atom. The experiments in toluene have shown that the thermal rearrangement under CO_2 to DMC was not operative, as opposed to that of Sn-1. Therefore, the successive stoichiometric events to DMC could be the involvement of methanol either as a provider of methoxy ligands leading to a dimethoxytin fragment or as reacting directly on a hemicarbonate $SnOC(O)OCH_3$ fragment.

4. Conclusions

The fixation of CO_2 to methanol for DMC synthesis was studied with $n\text{-}Bu_2Sn(OCH_3)_2$ over a range of conditions for getting mechanistic clues for better activity. The isolation and characterization, after catalytic runs, of a new molecular structure containing 10 tin atoms, formulated as $(n\text{-}Bu_2SnO)_6[(n\text{-}Bu_2SnOCH_3)_2(CO_3)]_2$, constitute a breakthrough in the mechanism understanding. The complex $n\text{-}Bu_2Sn(OCH_3)_2$ is prompted to form DMC, on a stoichiometric basis, via a thermal rearrangement to the deca-tin molecular complex, which is viewed as an organotin oxide species and considered as a resting species in the catalytic cycle. The preliminary kinetic study shows that the initial rate is higher with the stannane but the TONs are higher with the organotin oxide. Deactivation was evidenced due to reversible poisoning by H_2O formed in the carbonation of methanol reaction. Moreover, our results underline rate and turnover enhancements under monophasic supercritical conditions due to a positive order in CO_2. The reaction mechanism is considerably more complex than already reported. Currently, work is in progress to determine the rate-limiting step(s) and to correlate with in situ IR and NMR characterization of tin species under CO_2 pressure and temperature.

Supporting Information Available: selected bond lengths and angles for $(n\text{-}Bu_2SnO)_6[(n\text{-}Bu_2SnOCH_3)_2(CO_3)]_2$.

Acknowledgements

This work was supported by the Centre National de la Recherche Scientifique (France), the Ministère de la Recherche (France, R.L. grant), Fortum Foundation (Finland, H.T. grant), and Neste Jacobs (Finland).

Appendix A. Supplementary data

Supplementary data associated with this article can be found, in the online version, at doi:10.1016/j.cattod.2006.02.025.

References

[1] M. Aresta, A. Dibenedetto, Catal. Today 98 (2004) 455.
[2] H. Turunen, E. Pongracz, R. Keiski, in: Proceedings of the International Conference on Eco-Efficiency for Sustainability, Leiden, The Netherlands, 1–3 April, 2004.
[3] P. Licence, J. Ke, M. Sokolova, S.K. Ross, M. Poliakoff, Green Chem. 5 (2003) 99.
[4] E.J. Beckman, J. Supercrit. Fluids 28 (2004) 121.
[5] P.G. Jessop, W. Leitner (Eds.), Chemical Synthesis Using Supercritical Fluids, Wiley-VCH, Weinheim, 1999.
[6] Y. Guo, A. Akgerman, J. Supercrit. Fluids 15 (1999) 63.
[7] A. Baiker, Chem. Rev. 99 (1999) 453.
[8] W. Leitner, Acc. Chem. Res. 35 (2002) 746.
[9] P. Licence, W.K. Gray, M. Solokova, M. Poliakoff, J. Am. Chem. Soc. 127 (2005) 293.
[10] D. Ballivet-Tkatchenko, M. Picquet, M. Solinas, G. Francio, P. Wasserscheid, W. Leitner, Green Chem. 5 (2003) 232.
[11] W. Leitner, Pure Appl. Chem. 76 (2004) 635.
[12] M. Solinas, J. Jiang, O. Stelzer, W. Leitner, Angew. Chem. Int. Ed. 44 (2005) 2291.
[13] P.B. Webb, T.E. Kunene, D.J. Cole-Hamilton, Green Chem. 7 (2005) 373.
[14] W. Leitner, E. Dinjus, F. Gassner, J. Organomet. Chem. 475 (1994) 257.
[15] P.G. Jessop, Y. Hsiao, T. Ikariya, R. Noyori, J. Am. Chem. Soc. 118 (1996) 344.
[16] M. Rohr, J.-D. Grunwaldt, A. Baiker, J. Mol. Catal. A 226 (2005) 253.
[17] L. Schmid, M. Rohr, A. Baiker, Chem. Commun. (1999) 2303.
[18] O. Kröcher, R.A. Köppel, A. Baiker, Chem. Commun. (1997) 453.
[19] P.G. Jessop, T. Ikariya, R. Noyori, Chem. Rev. 99 (1999) 475.
[20] M. Aresta, A. Dibenedetto, C. Dileo, I. Tommasi, E. Amodio, J. Supercrit. Fluids 25 (2003) 177.
[21] H. Kawanami, A. Sasaki, K. Matsui, Y. Ikushima, Chem. Commun. (2003) 896.
[22] J. Kizlink, I. Pastucha, Collect. Czech. Chem. Commun. 59 (1994) 2116.
[23] A. Wagner, W. Löffler, B. Haas, DE Patent 4,310,109 to RWE. Chem. Abstr. 122 (1994) 186964.
[24] N.S. Isaacs, B. O'Sullivan, C. Verhaelen, Tetrahedron 55 (1999) 11949.
[25] T. Sakakura, J.-C. Choi, Y. Saito, T. Masuda, T. Sako, T. Oriyama, J. Org. Chem. 64 (1999) 4506.
[26] D. Ballivet-Tkatchenko, O. Douteau, S. Stutzmann, Organometallics 19 (2000) 4563.
[27] K. Tomishige, T. Sakaihori, Y. Ikeda, K. Fujimoto, Catal. Lett. 58 (1999) 225.
[28] D. Ballivet-Tkatchenko, T. Jerphagnon, R. Ligabue, L. Plasseraud, D. Poinsot, Appl. Catal. A 255 (2003) 93.
[29] P. Tundo, M. Selva, Acc. Chem. Res. 35 (2002) 706.
[30] F. Rivetti, C. R. Acad. Sci. Paris, Chem. 3 (2000) 497.
[31] M.A. Pacheco, C.L. Marshall, Energy Fuels 11 (1997) 2.
[32] F. Rivetti, U. Romano, D. Delledonne, in: P.T. Anastas, T.C. Williamson (Eds.), Green Chemistry, ACS Symposium Series 626, 1996, Chapter 6, p. 70.
[33] Y. Katrib, G. Deiber, P. Mirabel, S. Le Calvé, C. George, A. Mellouki, G. Le Bras, J. Atmos. Chem. 43 (2002) 151.
[34] Société Nationale des Poudres et Explosifs, FR Patent 2,163,884. Chem. Abstr. 80 (1973) 3112.
[35] D. Delledonne, F. Rivetti, U. Romano, Appl. Catal. A 221 (2001) 241.
[36] S. Uchiumi, K. Ataka, T. Matsuzaki, J. Organomet. Chem. 576 (1999) 279.
[37] D. Ballivet-Tkatchenko, S. Sorokina, in: M. Aresta (Ed.), Carbon Dioxide Recovery and Utilization, Kluwer Pub., Dordrecht, 2003 , p. 261 (Chapter 10).

[38] B.M. Trost, Angew. Chem. Int. Ed. 34 (1995) 259.
[39] T. Sakakura, J.-C. Choi, Y. Saito, T. Sako, Polyhedron 19 (2000) 573.
[40] K.T. Jung, A.T. Bell, Top. Catal. 20 (2002) 97.
[41] M. Aresta, A. Dibenedetto, C. Pastore, Inorg. Chem. 42 (2003) 3256.
[42] D.F. Shriver, The Manipulation of Air-Sensitive Compounds, McGraw-Hill, New York, 1986.
[43] G.-L. Zeng, J.-F. Ma, J. Yang, Y.-Y. Li, X.-R. Hao, Chem. Eur. J. 10 (2004) 3761.
[44] P.J. Smith, A.P. Tupciauskas, Ann. Rep. NMR Spectrosc. 8 (1978) 291.
[45] T.E. Daubert, R.P. Danner, Physical and Thermodynamic Properties of Pure Chemicals, Part 1, Hemisphere Pub. Corp, New York, 1989.
[46] E. Brunner, W. Hueltenschmidt, G. Schlichthaerle, J. Chem. Therm. 19 (1987) 273.
[47] S.-D. Yeo, S.-J. Park, J.-W. Kim, J.-C. Kim, J. Chem. Eng. Data 45 (2000) 932.
[48] J. Liu, Z. Qin, G. Wang, X. Hou, J. Wang, J. Chem. Eng. Data 48 (2003) 1610.
[49] I. Polishuk, J. Wisniak, H. Segura, Chem. Eng. Sci. 56 (2001) 6485.
[50] K.I. Keskinen, J. Aittamaa, FLOWBAT, User's Instruction Manual, Espoo, 2005.
[51] G. Soave, Chem. Eng. Sci. 27 (1972) 1197.
[52] J.O. Valderrama, Ind. Eng. Chem. Res. 42 (2003) 1603.
[53] W.O. Morris, M.D. Donohue, J. Chem. Eng. Data 30 (1985) 259.